OPEN ACCESS

Unveiling the Thermal Stability of Sodium Ion Pouch Cells Using Accelerating Rate Calorimetry

Journal of The Electrochemical Society, 2024 **171** 070512

Unveiling the Thermal Stability of Sodium Ion Pouch Cells Using Accelerating Rate Calorimetry

Chanmonirath (Michael) Chak,[1,2] Rishivandhiga Jayakumar,[1,2] Vadim Shipitsyn,[1,2] Ean Bass,[1,2] Reece McCloskey,[1,2] Wenhua Zuo,[3] Phung M. L. Le,[4,z] Jun Xu,[5,z] and Lin Ma[1,2,z]

[1]*Department of Mechanical Engineering and Engineering Science, The University of North Carolina at Charlotte, Charlotte, North Carolina 28223, United States of America*
[2]*Battery Complexity, Autonomous Vehicle and Electrification (BATT CAVE) Research Center, The University of North Carolina at Charlotte, Charlotte, North Carolina 28223, United States of America*
[3]*Chemical Sciences and Engineering Division, Argonne National Laboratory, Lemont, Illinois 60439, United States of America*
[4]*Energy and Environment Directorate, Pacific Northwest National Laboratory, Richland, Washington 99352, United States of America*
[5]*Department of Mechanical Engineering, University of Delaware, Newark, Delaware 19716, United States of America*

The thermal stability of ~420 mAh $Na_{0.97}Ca_{0.03}[Mn_{0.39}Fe_{0.31}Ni_{0.22}Zn_{0.08}]O_2$ (NCMFNZO)/hard carbon (HC) pouch cells was investigated using accelerating rate calorimetry (ARC) at elevated temperatures. 1 m $NaPF_6$ in propylene carbonate (PC):ethyl methyl carbonate (EMC) (1:1 by volume) was used as a control electrolyte. Adding 2 wt% fluoroethylene carbonate to the electrolyte improves the cell's thermal stability by decreasing the self-heating rate (SHR) across the whole testing temperature range. The selected states-of-charge (SoC), including 70%, 84%, and 100%, exhibit minimal impact on the exothermic behavior, except for a slight decrease in SHR after ~275 °C at 70% SoC. When compared to traditional lithium-ion batteries operating at 100% SoC, NCMFNZO/HC pouch cells demonstrate inferior thermal stability compared to $LiFePO_4$ (LFP)/graphite pouch cells, displaying a higher SHR from 220 to 300 °C. $LiNi_{0.8}Mn_{0.1}Co_{0.1}O_2$/graphite + SiO_x pouch cells exhibit the worst safety performance, with an early onset temperature of ~100 °C and the highest SHR across the entire temperature range. These results offer a direct comparison of the impact of SoC and electrolyte compositions on the thermal stability of SIBs at elevated temperatures, highlighting that there is still room for improvement in SIBs safety performance compared to LFP/graphite chemistry.

 [DOI: 10.1149/1945-7111/ad5e00]

Manuscript submitted May 10, 2024; revised manuscript received June 12, 2024. Published July 10, 2024.

In recent years, there has been a considerable surge in interest in sodium-ion batteries (SIBs), driven largely by the abundant supply and relatively lower cost of sodium compared to lithium.[1,2] Cathode active materials commonly used in SIBs include layered transition metal oxides[3–7] (e.g., Na_xMO_2, M = Mn, Fe, Ni, Cu, etc.), polyanionic compounds[8,9] (e.g. $NaFePO_4$), and Prussian blue analogues (PBAs)[10,11] such as $Na_xFeFe(CN)_6$ and $Na_xMnFe(CN)_6$, which rely on Earth-abundant elements such as Fe and Cu, enhancing the attractiveness of SIB technology. While SIBs are increasingly favored by researchers as a promising power source for grid energy storage systems and low-speed electric vehicles (EVs), safety concerns may erode consumer confidence and hinder widespread adoption. Therefore, further investigation into the safety issues of SIBs is warranted.

The reasons for battery exothermal behavior and safety-related issues can be traced back to the reactions between charged electrodes and electrolytes under abusive conditions such as elevated temperatures.[12] Accelerating rate calorimetry (ARC) is a valuable method for studying exothermic chemical reactions in conditions that mimic adiabatic environments.[13–15] Through ARC, crucial parameters including onset temperature, self-heating rate (SHR), and temperature rise can be determined to characterize the exothermic process. Extensive efforts have been dedicated to using ARC to understand the exothermic processes of SIB components at the material level. Xia et al.[16] demonstrated that sodiated hard carbon (HC) anode exhibits higher reactivity with dimethyl carbonate (DMC) and diethyl carbonate (DEC) compared to ethylene carbonate (EC). Xia et al.[17] found that sodiated HC anode shows increased reactivity in $NaPF_6$/EC: DEC electrolyte compared to EC: DEC due to the high thermal stability of $NaPF_6$, preventing the formation of NaF, and the preferential solvation of $NaPF_6$ by EC, leading to enhanced reaction with DEC. Furthermore, Xia et al.[18] reported that de-sodiated $NaCrO_2$ exhibits unexpectedly excellent thermal stability in solvents without releasing heat within the ARC test temperature range due to minimal oxygen release. By combining ARC with X-ray diffraction (XRD), Xia et al.[19] uncovered that de-sodiated $NaNi_{0.5}Mn_{0.5}O_2$ decomposes at elevated temperatures up to 300 °C to produce nickel manganese oxide and Ni metal, with the released oxygen reacting with the solvent.

To significantly enhance the lifespan of SIBs and promote their widespread adoption as a viable alternative to lithium-ion batteries (LIBs), extensive research has been conducted on electrolyte engineering and controlling the upper cut-off voltage. These efforts aim to enhance the characteristics of the electrode-electrolyte interphase (EEI) and mitigate side reactions. Shipitsyn et al.[20] showed that the addition of fluoroethylene carbonate (FEC) additive can improve the capacity retention of $Na_{0.97}Ca_{0.03}[Mn_{0.39}Fe_{0.31}Ni_{0.22}Zn_{0.08}]O_2$ (NCMFNZO)/HC pouch cells up to 90% after 200 cycles with C/3 at 40 °C. Jin et al.[21] presented a low-solvation electrolyte comprising 1.5 M sodium bis (fluorosulfonyl)imide (NaFSI) salt in a solvent mixture of DMC and tris(2,2,2-trifluoroethyl) phosphate (TFP) (1.5:2 in mole), aimed at reducing EEI dissolution and extending the lifetime of $NaNi_{0.68}Mn_{0.22}Co_{0.1}O_2$/HC cells, achieving >90% capacity retention after 300 cycles at 4.2 V. Hijazi et al.[22] revealed that by lowering the upper cut-off voltage from 4.0 V to 3.8 V, long-lasting SIBs exhibiting 97% capacity retention after 450 cycles at 40 °C could be achieved. Nevertheless, the trade-off between thermal stability and longevity has received limited attention when applying these strategies at the cell level.

In this work, we examined the thermal stability of ~420 mAh NCMFNZO/HC pouch cells using ARC under elevated temperatures from 50 °C to 300 °C. We investigated the impact of different

[z]E-mail: phung.le@pnnl.gov; junxu@udel.edu; l.ma@charlotte.edu

electrolyte compositions by varying the concentrations of the FEC additive. Additionally, we tested the thermal stability of the cells at three different states-of-charge (SoCs): 70%, 84%, and 100%, to assess the influence of SoC on cell performance. Furthermore, we compared the safety performance of these cells with typical lithium-ion batteries (LIBs), including $LiFePO_4$ (LFP)/graphite and $LiNi_{0.8}Mn_{0.1}Co_{0.1}O_2$/graphite + SiO_x pouch cells, all tested at 100% SoC.

Experimental

Electrode and electrolyte preparation.—Machine-made 210 mAh NCMFNZO/HC pouch cells, 240 mAh LFP/graphite pouch cells, and 240 mAh NMC811/graphite + SiO_x pouch cells, without electrolyte, were obtained from Lifun Technology (Zhuzhou, Hunan, China). In NCMFNZO/HC pouch cells, the cathode consists of 95 wt % NCMFNZO active material, 3 wt% carbon black, and 2 wt% polyvinylidene fluoride (PVDF) binder, while the anode comprises 95 wt% HC active material and 5 wt% binder. The areal loadings of the cathode and anode are 16 mg cm^{-2} and 9.47 mg cm^{-2}, respectively, with both electrodes utilizing aluminum foil as the current collector. In LFP/graphite pouch cells, the cathode is composed of 96.5 wt% LFP active material, 1.5 wt% carbon black, and 2 wt% PVDF binder, while the anode consists of 95.7 wt% graphite active material, 3 wt% carboxymethyl cellulose/styrene–-butadiene rubber (CMC/SBR) binder, and 1.3 wt% carbon black. The areal loadings of the cathode and anode are 17.03 mg cm^{-2} and 8.51 mg cm^{-2}, respectively. For NMC811/graphite + SiO_x pouch cells, the cathode contains 96.4 wt% NMC811 active material, 1.6 wt% carbon black, and 2 wt% PVDF binder, while the anode is comprised of 94.0 wt% graphite + SiO_x active material, 5 wt% CMC/SBR binder, and 1.0 wt% carbon black. The weight ratio between graphite and SiO_x is 4:1. The areal loadings of the cathode and anode are 14.96 mg cm^{-2} and 7.72 mg cm^{-2}, respectively.

In this study, a control electrolyte for NCMFNZO/HC pouch cells consisted of 1 m $NaPF_6$ (>98.0%, TCI) in PC (H_2O < 20 ppm, Gotion) mixed with ethyl methyl carbonate (EMC, H_2O < 20 ppm, Gotion) in a 1:1 volume ratio. Electrolytes with additives were prepared by dissolving FEC (H_2O < 20 ppm, Gotion) into the control electrolyte in various ratios. 1 m $LiPF_6$ in EC/EMC 3/7 (by vol., Gotion) was used as the electrolyte in LFP/graphite pouch cells. 1 m $LiPF_6$ in EC/EMC 3/7 (by vol., Gotion) + 10 wt% FEC was used as the electrolyte in NMC811/graphite + SiO_x pouch cells.

Electrochemical formation and preparation.—The dry pouch cells were filled with 1 g of electrolyte and vacuum-sealed using a compact vacuum sealer (MSK-115A-111, MTI Cor.) under a pressure gauge of −90 kPa with a sealing temperature of 165 °C and a sealing time of 5 seconds inside an Ar-filled glove box. During the formation step of NCMFNZO/HC pouch cells, all cells were transferred to temperature-controlled chambers (Neware Battery Testing System, Shenzhen, China) set at 40 ± 0.1 °C and allowed to rest for 3 h before charging to 4 V at a rate of C/20. Subsequently, the cells were discharged to 3.1 V at a rate of C/20 for the degas step. During formation, LFP/graphite pouch cells were charged to 1.5 V, rested for 10 hours, then charged to 3.65 V, while NMC811/graphite + SiO_x pouch cells were charged to 1.5 V, rested for 10 hours, then charged to 4.2 V, both at a rate of C/20 and 40 ± 0.1 °C. LFP/

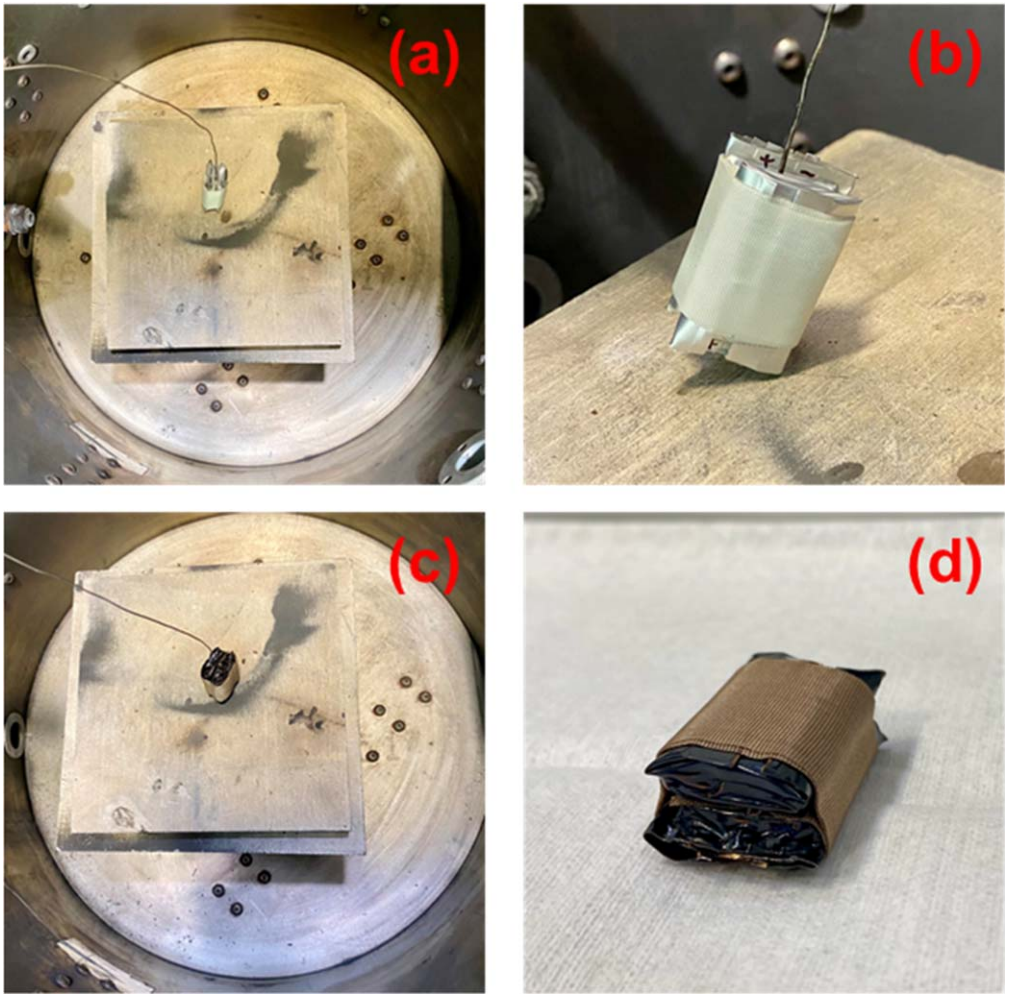

Figure 1. A summary of pictures of a pair of pouch cells before ARC testing (a)–(b) and after ARC testing (c)–(d).

graphite and NMC811/graphite + SiO_x pouch cells were then discharged to 2.6 V and 3.8 V, respectively, using C/20 for degas.

After degassing, NCMFNZO/HC pouch cells were charged to different upper cut-off voltages (3.6 V, 3.8 V, and 4 V) using C/20, followed by holding at 4 V until the current reached C/200, to prepare cells with different states of charge for subsequent ARC characterizations. To attain 100% SoC for ARC testing, LFP/graphite and NMC811/graphite + SiO_x pouch cells were charged to 3.65 V and 4.2 V, respectively, at a rate of C/20 until the current reached C/200.

Accelerating rate calorimetry (ARC) measurements.—Using glass tape, two pouch cells were wrapped around the thermocouple of an accelerating rate calorimeter (EV+, Thermal Hazard Technology) during each test. The thermocouple remained attached in the center between the two pouch cells throughout the entire testing period (Fig. 1). ARC testing was monitored under adiabatic conditions when the sample's self-heating rate (SHR) surpassed 0.02 °C min^{-1}. Data collection for ARC was conducted within the temperature range of 50 °C to 315 °C. The heating step was set as 5.0 °C/step. Experiments were programmed to automatically stop when the temperature exceeded 350 °C or if the SHR exceeded 10 ° C min^{-1}.

Since gas venting, which depends on both electrode and electrolyte chemistries, could affect ARC results, the temperatures at which gas venting occurred were examined using NCMFNZO/HC and NMC811/graphite + SiO_x pouch cells as examples. For NCMFNZO/HC pouch cells, gas venting occurred at approximately 180 °C (Fig. 2a), whereas for NMC811/graphite + SiO_x pouch cells, it occurred at around 100 °C (Fig. 2b).

Results and Discussion

Figures 3a–3e show the weight and dimension information of one sodium-ion cell used in this study. Calculating with an integrated energy of 0.784 Wh during the first formation cycle at 40 °C (Fig. 3f), the gravimetric and volumetric energy densities for a single cell are 153.1 Wh kg^{-1} and 248.9 Wh l^{-1}, respectively, when charged to 4.0 V. Despite an initial charging capacity of ∼250 mAh (Fig. 3f), irreversible capacity loss leads to a reversible capacity of ∼210 mAh, as observed in previous research.[20] Therefore, we state that ARC testing was carried out on approximately ∼420 mAh cells in this study, with two cells subjected to ARC analysis.

FEC has been widely used as an electrolyte additive in SIBs to extend cell lifetime. Here its effect on the thermal stability of sodium-ion pouch cells was carefully characterized using ARC. The pouch cells ARC behavior results from the interactions between the cathode, anode, and electrolytes at elevated temperatures. Based on our previous ARC study at the material level,[20] adding FEC has minimal effect on the reactions between de-sodiated NCMFNZO cathode and electrolytes at elevated temperatures. However, the addition of FEC can suppress SHR between sodiated HC anode and electrolytes at high temperatures. Therefore, the differences observed in the ARC results of full pouch cells likely originate from the HC anode side. Figure 4 shows the SHR versus temperature results on NCMFNZO/HC pouch cells at 4.0 V (equivalent to100% SoC, Fig. 3f) while utilizing different amounts of FEC additive. It's worth noting that each experiment underwent replication, yielding highly reproducible outcomes. Figure 4 shows there is almost no obvious heat release until ∼165 °C for NCMFNZO/HC pouch cells with 1 m $NaPF_6$ in PC/EMC 1/1 (by vol.) as the control electrolyte. However, the SHR dramatically increases above ∼210 °C. The introduction of 2 wt% FEC maintains the onset temperature at ∼165 °C, consistent with the control electrolyte, yet displays a reduced SHR beyond the threshold of ∼190 °C in comparison to the control. When the FEC content is increased to 5 wt%, a slight exothermic response is observed from ∼90 °C to ∼165 °C, possibly due to reactions between the HC anode and electrolyte, as reported in prior studies.[20] Beyond 165 °C, the samples containing 5 wt% FEC demonstrate a performance similar to those with 2 wt% FEC, exhibiting a reduced SHR compared to the control sample. As a side note, 2 wt% FEC containing cells show an initial decrease in SHR at ∼180 °C, which could be attributed to gas venting (Fig. 2a).

In this study, charging the NCMFNZO/HC pouch cells to 4.0 V is considered as reaching 100% SoC. When adjusting the SoC by reducing the upper cut-off voltage to 3.8 V (equivalent to ∼84% SoC) and 3.6 V (equivalent to ∼70% SoC), a loss of 20.03% and 35.84% in energy or energy density is observed (Fig. 3f). Despite the decrease in energy density, previous research suggests that extending the SIBs lifetime can be achieved by mitigating side reactions between the cathode and electrolyte.[22] Therefore, studying the effect of SoC on the thermal stability of SIBs presents an intriguing avenue for further investigation. Figure 5 shows the SHR versus temperature results on NCMFNZO/HC pouch cells at different SoCs including 100%, 84% and 70% while the electrolyte of 1 m $NaPF_6$ in PC/EMC 1/1 (by vol.) + 2 wt% FEC was used. Surprisingly, the chosen SoCs do not exhibit a significant effect on the exothermal behavior of NCMFNZO/HC pouch cells. Only a minor difference is noticeable after 270 °C, where the selection of 70% SoC demonstrates a smaller SHR compared to 84% and 100% SoC.

To position the thermal stability of SIBs relative to other lithium-ion batteries (LIBs), we selected two types of typical LIBs: LFP/graphite and NMC811/graphite + SiO_x pouch cells (figures 6a–6e and 6g–6k), for comparison. LFP remains a focus for use in LIBs

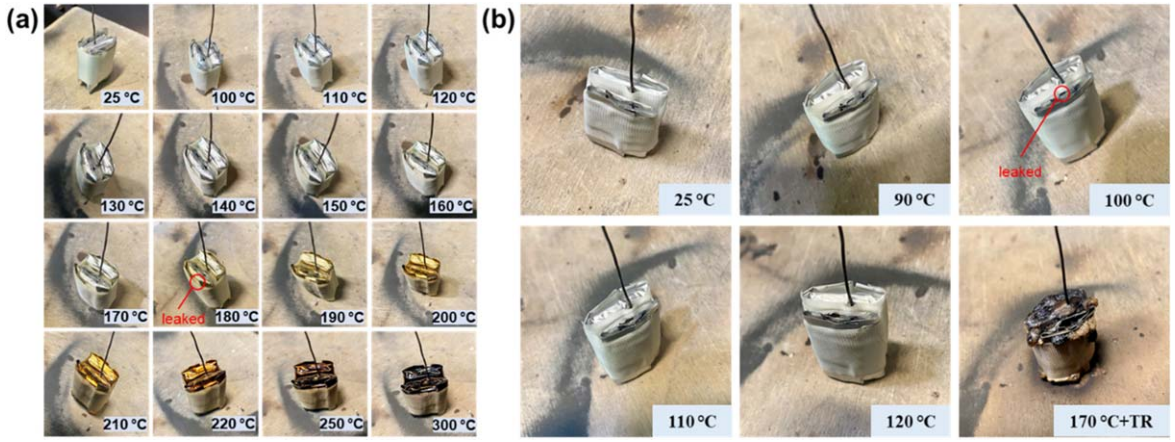

Figure 2. A summary of pictures of a pair of pouch cells during heating at different temperatures. Cells were hold at different temperatures for 30 min before taking the pictures. (a) NCMFNZO/HC pouch cells with 1 m $NaPF_6$ in PC/EMC 1/1 (by vol.) + 2 wt% FEC. Gas venting occurred at ∼180 °C. (b) NMC811/graphite + SiO_x pouch cells 1 m $LiPF_6$ in EC/EMC 3/7 + 10 wt% FEC. Gas venting occurred at ∼100 °C and cells went to thermal runaway (TR) after heating from 120 °C to 170 °C.

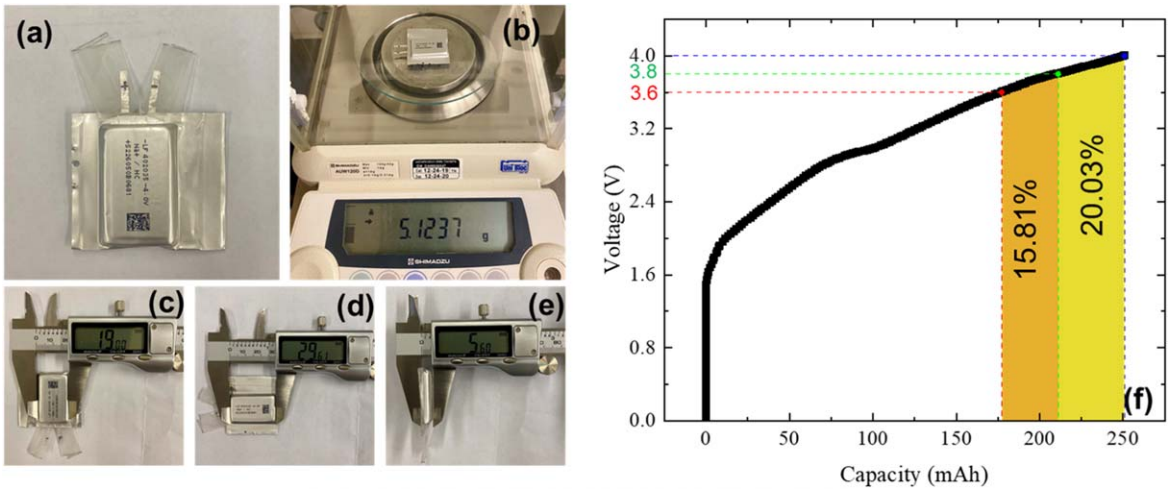

Figure 3. A summary of a sodium-ion cell information used for ARC testing. The appearance (a), weight (b), and dimension (c–e) of a single sodium-ion cell. (f) Voltage vs capacity of a sodium-ion cell when charging to 4.0 V with C/20 at 40 °C. The charge capacity is 250.8 mAh at 4.0 V, 211.2 mAh at 3.8 V, and 177.3 mAh at 3.6 V.

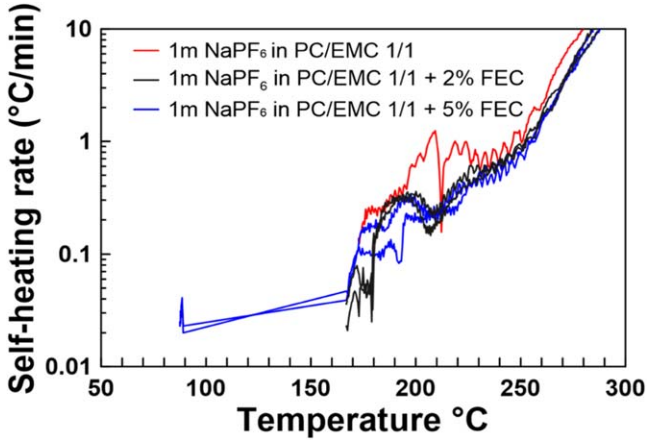

Figure 4. SHR vs temperature for NCMFNZO/HC pouch cells at 4.0 V (i.e. 100% SoC) with different electrolytes as labeled. Each ARC testing includes two ∼210 mAh pouch cells.

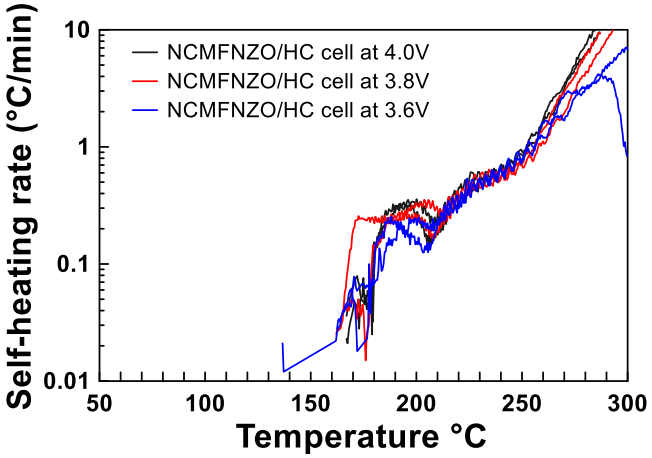

Figure 5. SHR vs temperature for NCMFNZO/HC pouch cells with 1 m $NaPF_6$ in PC/EMC 1/1 (by vol.) + 2 wt% FEC at different SoC as labeled. Each ARC testing includes two ∼210 mAh pouch cells.

because of its cost-effective and abundant precursor materials, as well as its excellent safety features.[23] At the same time, high nickel containing cathodes (e.g., NMC811[24]) and silicon containing anodes[25] have gained significant attention due to their potential to boost cell energy density. Charging the two types of cells to 3.65 V (Fig. 6f and 4.2 V (Fig. 6l), respectively, leads to achieving 100% SoC, with corresponding cell energies of 0.915 Wh and 1.0 Wh, as integrated (Figs. 6f and 6l). Leveraging the weight and dimensional data provided, we proceed to calculate the gravimetric and volumetric energy densities of these LIBs. The LFP/graphite pouch cell exhibits gravimetric and volumetric energy densities of 164.3 Wh kg^{-1} and 361.8 Wh l^{-1}, respectively, while the NMC811/graphite + SiO_x pouch cell demonstrates gravimetric and volumetric energy densities of 232.6 Wh kg^{-1} and 540.1 Wh l^{-1}, respectively. Traditional electrolyte consisting of 1 m $LiPF_6$ in EC/EMC 3/7 was utilized in LFP/graphite pouch cells, whereas a deliberate addition of 10 wt% FEC additive was made to the electrolyte for NMC811/graphite + SiO_x pouch cells due its widespread adoption for the purpose of extending cell lifetime.[26,27] ARC testing for these LIBs was conducted at 100% SoC to compare results with those from SIBs.

Figure 7 shows the SHR versus temperature results on NCMFNZO/HC, LFP/graphite, and NMC811/graphite + SiO_x pouch cells when all the cells were at 100% SoC. Apart from some minor exothermic behavior observed before ∼165 °C, the LFP/graphite cell exhibits superior thermal stability compared to the NCMFNZO/HC cell, as evidenced by a smaller SHR from ∼165 °C to 300 °C. Throughout the entire testing temperature range, the SHR of LFP/graphite cells has consistently remained below 0.5 °C min^{-1}. As a result of the well-known thermal instability issue with high nickel containing cathodes,[13] NMC811/graphite + SiO_x pouch cells exhibit markedly greater reactivity compared to other samples across all temperature ranges, with an early onset temperature of ∼100 °C. Its SHR shows a slight decrease at ∼104 °C, likely due to gas venting (Fig. 2b). Its SHR is above 10 °C min^{-1} when the temperature is only ∼175 °C. This suggests the use of NMC811/graphite + SiO_x pouch cells might not be advisable from a safety performance standpoint, despite their advantage of offering higher energy density.

Conclusions

In this work, leveraging ∼420 mAh NCMFNZO/HC pouch cells as testing vehicles, the effect of electrolyte compositions and SoC on the thermal stability of SIBs was studied using ARC. With a similar onset temperature at ∼165 °C, the use of 2 wt% FEC additive resulted in a lower SHR from ∼165 °C to 300 °C compared to the control electrolyte. Although showing a function of suppressing

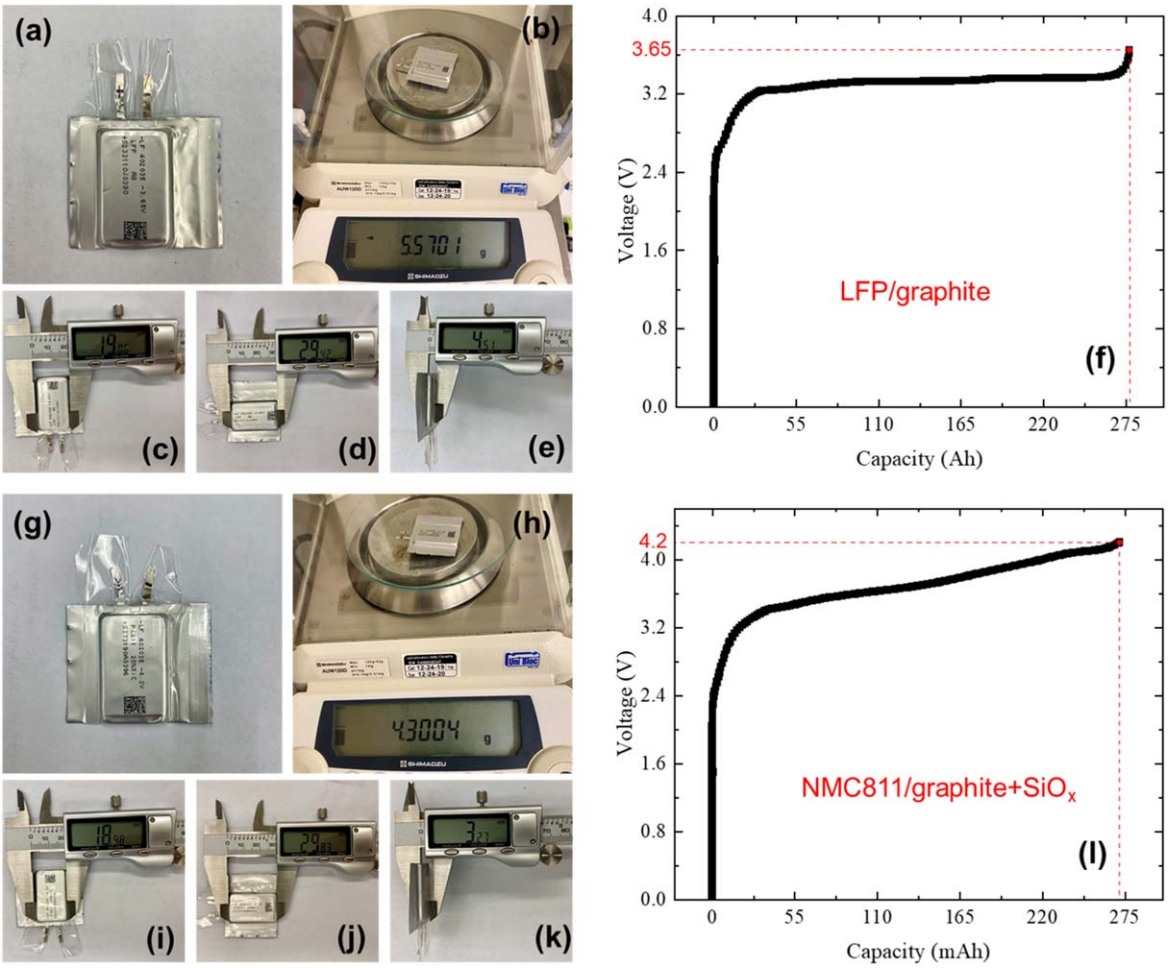

Figure 6. A summary of a lithium-ion cell information used for ARC testing. The appearance (a), weight (b), and dimension (c)–(e) of a single LFP/graphite pouch cell. (f) Voltage vs capacity of a LFP/graphite pouch cell when charging to 3.65 V with C/20 at 40 °C. The charge capacity is 277.4 mAh at 3.65 V. The appearance (g), weight (h), and dimension (i)–(k) of a single NMC811/graphite + SiO_x pouch cell. (f) Voltage vs capacity of a NMC811/graphite + SiO_x pouch cell when charging to 4.2 V with C/20 at 40 °C. The charge capacity is 271.5 mAh at 4.2 V.

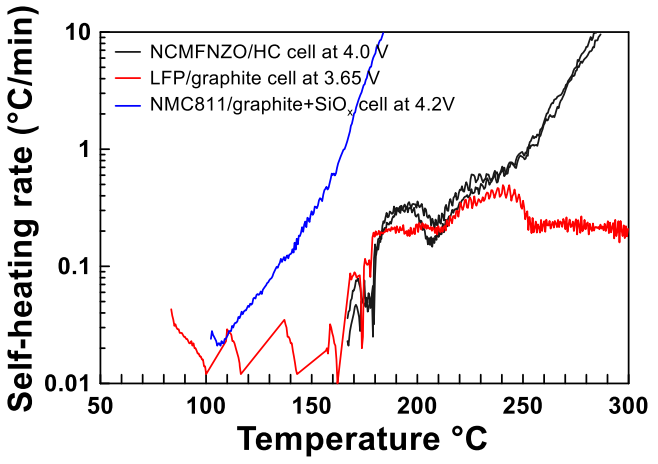

Figure 7. SHR vs temperature for NCMFNZO/HC pouch cells with 1 m $NaPF_6$ in PC/EMC 1/1 (by vol.) + 2 wt% FEC at 4.0 V, LFP/graphite pouch cells with 1 m $LiPF_6$ in EC/EMC 3/7 (by vol.) at 3.65 V, and NMC811/graphite+SiOx pouch cells with 1 m $LiPF_6$ in EC/EMC 3/7 (by vol.) + 10 wt % FEC at 4.2 V. Each ARC testing includes two pouch cells.

SHR beyond ∼165 °C, the use of 5 wt% FEC shows a trivial exothermic behavior from ∼90 °C to ∼165 °C. The use of suitable amount of FEC additive is able to improve SIBs safety performance, which is consistent with previous ARC studies[20] at materials level. Regarding the effect of SoC, three SoCs including 100%, 84%, and 70% demonstrates very similar exothermic performance across the whole temperature range from 50 °C to 300 °C, except for a slight SHR decrease after 270 °C from 70% SoC. This indicates a trivial trade-off between high energy density and safety in SIBs. The safety performance under elevated temperatures was also compared between NCMFNZO/HC, LFP/graphite, and NMC811/graphite + SiO_x pouch cells, all at 100% SoC. NCMFNZO/HC pouch cells exhibited inferior performance compared to LFP/graphite pouch cells, displaying a higher SHR after 250 °C. However, NCMFNZO/HC pouch cells showed much better performance compared to NMC811/graphite + SiO_x pouch cells, which had an early onset temperature of ∼100 °C.

This study offers significant insights into the safety performance of SIBs at the cell level when layered transition metal oxide is employed as the cathode material. Further research is required to comprehend the impact of other types of cathodes, including Prussian blue analogs and polyanion-based ones, on the safety performance of SIBs at elevated temperatures. This is crucial prior to the large-scale deployment of SIBs in grid energy storage systems.

Acknowledgments

Lin Ma at UNC Charlotte acknowledges the support by the US National Science Foundation Award No. 2301719 and ORAU Ralph

E. Powe Junior Faculty Enhancement Award. There are no conflicts to declare.

ORCID

Jun Xu https://orcid.org/0000-0002-8619-8737
Lin Ma https://orcid.org/0000-0003-1183-1347

References

1. H. S. Hirsh, Y. Li, D. H.-S. Tan, M. Zhang, E. Zhao, and Y. S. Meng, "Sodium-ion batteries paving the way for grid energy storage." *Adv. Energy Mater.*, **10**, 2001274 (2020).
2. J.-Y. Hwang, S.-T. Myung, and Y.-K. Sun, "Sodium-ion batteries: present and future." *Chem. Soc. Rev.*, **46**, 3529 (2017).
3. E. Boivin, R. A. House, J.-J. Marie, and P. G. Bruce, "Controlling iron versus oxygen redox in the layered cathode $Na_{0.67}Fe_{0.5}Mn_{0.5}O_2$: mitigating voltage and capacity fade by Mg substitution." *Adv. Energy Mater.*, **12**, 2200702 (2022).
4. R. J. Clément, P. G. Bruce, and C. P. Grey, "Review—Manganese-based P2-Type transition metal oxides as sodium-ion battery cathode materials." *J. Electrochem. Soc.*, **162**, A2589 (2015).
5. Z. Li, W. Kong, Y. Yu, J. Zhang, D. Wong, Z. Xu, Z. Chen, C. Schulz, M. Bartkowiak, and X. Liu, "Tuning bulk O_2 and nonbonding oxygen state for reversible anionic redox chemistry in P2-Layered cathodes." *Angew. Chem. Int. Ed.*, **61**, e202115552 (2022).
6. H. Liu et al., "Reversible Op4 phase in P2–$Na_{2/3}Ni_{1/3}Mn_{2/3}O_2$ sodium ion cathode." *J. Power Sources*, **508**, 230324 (2021).
7. J. Liu, C. Didier, M. Sale, N. Sharma, Z. Guo, V. K. Peterson, and C. D. Ling, "Elucidation of the high-voltage phase in the layered sodium ion battery cathode material P3–$Na_{0.5}Ni_{0.25}Mn_{0.75}O_2$." *J. Mater. Chem. A*, **8**, 21151 (2020).
8. C. Berlanga, I. Monterrubio, M. Armand, T. Rojo, M. Galceran, and M. Casas-Cabanas, "Cost-effective synthesis of triphylite-Nafepo4 cathode: a zero-waste process." *ACS Sustainable Chemistry & Engineering*, **8**, 725 (2020).
9. W. Tang et al., "High-performance Nafepo4 formed by aqueous ion-exchange and its mechanism for advanced sodium ion batteries." *J. Mater. Chem. A*, **4**, 4882 (2016).
10. Y. Liu, Y. Qiao, W. Zhang, Z. Li, X. Ji, L. Miao, L. Yuan, X. Hu, and Y. Huang, "Sodium storage in Na-Rich $Na_xFeFe(CN)_6$ nanocubes." *Nano Energy*, **12**, 386 (2015).
11. Y. P. Wang, B. P. Hou, X. R. Cao, S. Q. Wu, and Z. Z. Zhu, "Structural evolution, redox mechanism, and ionic diffusion in rhombohedral $Na_2FeFe(CN)_6$ for sodium-ion batteries: first-principles calculations." *J. Electrochem. Soc.*, **169**, 010525 (2022).
12. H. Jia et al., "Is nonflammability of electrolyte overrated in the overall safety performance of lithium ion batteries? a sobering revelation from a completely nonflammable electrolyte." *Adv. Energy Mater.*, **13**, 2203144 (2023).
13. L. Ma, M. Nie, J. Xia, and J. R. Dahn, "A systematic study on the reactivity of different grades of charged $Li[Ni_xMn_yCo_z]O_2$ with electrolyte at elevated temperatures using accelerating rate calorimetry." *J. Power Sources*, **327**, 145 (2016).
14. L. Ma, J. Xia, X. Xia, and J. R. Dahn, "The impact of vinylene carbonate, fluoroethylene carbonate and vinyl ethylene carbonate electrolyte additives on electrode/electrolyte reactivity studied using accelerating rate calorimetry." *J. Electrochem. Soc.*, **161**, A1495 (2014).
15. Y. Wang, J. Jiang, and J. R. Dahn, "The reactivity of delithiated $Li(Ni_{1/3}Co_{1/3}Mn_{1/3})O_2$, $Li(Ni_{0.8}Co_{0.15}Al_{0.05})O_2$ or $LiCoO_2$ with non-aqueous electrolyte." *Electrochem. Commun.*, **9**, 2534 (2007).
16. X. Xia and J. R. Dahn, "Study of the reactivity of Na/Hard carbon with different solvents and electrolytes." *J. Electrochem. Soc.*, **159**, A515 (2012).
17. X. Xia, M. N. Obrovac, and J. R. Dahn, "Comparison of the reactivity of Na_xC_6 and Li_xC_6 with non-aqueous solvents and electrolytes." *Electrochem. Solid-State Lett.*, **14**, A130 (2011).
18. X. Xia and J. R. Dahn, "$NaCrO_2$ is a fundamentally safe positive electrode material for sodium-ion batteries with liquid electrolytes." *Electrochem. Solid-State Lett.*, **15**, A1 (2011).
19. X. Xia and J. R. Dahn, "A study of the reactivity of de-intercalated $NaNi_{0.5}Mn_{0.5}O_2$ with non-aqueous solvent and electrolyte by accelerating rate calorimetry." *J. Electrochem. Soc.*, **159**, A1048 (2012).
20. V. Shipitsyn, R. Jayakumar, W. Zuo, W. Yin, E. Huber, and L. Ma, "The impact of fluoroethylene carbonate additive on charged sodium ion electrodes/electrolyte reactivity studied using accelerating rate calorimetry." *J. Electrochem. Soc.*, **170**, 110501 (2023).
21. Y. Jin et al., "Low-solvation electrolytes for high-voltage sodium-ion batteries." *Nat. Energy*, **7**, 718 (2022).
22. H. Hijazi, Z. Ye, L. Zhang, J. Deshmukh, M. B. Johnson, J. R. Dahn, and M. Metzger, "Impact of sodium metal plating on cycling performance of layered oxide/hard carbon sodium-ion pouch cells with different voltage cut-offs." *J. Electrochem. Soc.*, **170**, 070512 (2023).
23. J. Jiang and J. R. Dahn, "Arc studies of the thermal stability of three different cathode materials: $LiCoO_2$; $Li[Ni_{0.1}Co_{0.8}Mn_{0.1}]O_2$; and Lifepo4, in $LiPF_6$ and LiBOB EC/DEC electrolytes." *Electrochem. Commun.*, **6**, 39 (2004).
24. A. Eldesoky, M. Bauer, S. Azam, E. Zsoldos, W. Song, R. Weber, S. Hy, M. B. Johnson, M. Metzger, and J. R. Dahn, "Impact of graphite materials on the lifetime of NMC811/graphite pouch cells: Part I. Material properties, arc safety tests, gas generation, and room temperature cycling." *J. Electrochem. Soc.*, **168**, 110543 (2021).
25. A. J. Louli, J. Li, S. Trussler, C. R. Fell, and J. R. Dahn, "Volume, pressure and thickness evolution of li-ion pouch cells with silicon-composite negative electrodes." *J. Electrochem. Soc.*, **164**, A2689 (2017).
26. R. Petibon, V. L. Chevrier, C. P. Aiken, D. S. Hall, S. R. Hyatt, R. Shunmugasundaram, and J. R. Dahn, "Studies of the capacity fade mechanisms of $LiCoO_2$/Si-Alloy: graphite cells." *J. Electrochem. Soc.*, **163**, A1146 (2016).
27. N. Zhang, S. Yu, I. Hamam, B. Tang, M. Johnson, and J. R. Dahn, "Long-term cycling and mechanisms of cell degradation of single crystal $LiNi_{0.95}Mn_{0.04}Co_{0.01}O_2$/graphite cells." *J. Electrochem. Soc.*, **171**, 010520 (2024).